ELSEVIER

Journal of Magnetism and Magnetic Materials 240 (2002) 86–91

Journal of magnetism and magnetic materials

www.elsevier.com/locate/jmmm

Criteria for ferromagnetic–insulator–ferromagnetic tunneling

Johan J. Åkerman[a,c,*], R. Escudero[a,d], C. Leighton[a], S. Kim[a], D.A. Rabson[b], Renu Whig Dave[c], J.M. Slaughter[c], Ivan K. Schuller[a]

[a] *Physics Department 0319, University of California, La Jolla, San Diego, CA 92093, USA*
[b] *Department of Physics, PHY 114, University of South Florida, Tampa, FL 33620, USA*
[c] *Motorola Labs, Physical Sciences Research Laboratories, Tempe, AZ 85284, USA*
[d] *IIM, Universidad Nacional Autonoma de Mexico, A Postal 70-360, Mexico, D.F. 04510, Mexico*

Abstract

The Rowell criteria, commonly used to identify tunneling in magnetic tunnel junctions (MTJ), are scrutinized. While neither the exponential-thickness dependence of the conductivity nor fits of non-linear transport data are found to be reliable tunneling criteria, the temperature-dependent conductivity does remain a solid criterion. Based on experimental studies of the bias and temperature-dependent resistance and magnetoresistance of MTJs, with and without shorted barriers, a new set of criteria is formulated. © 2002 Elsevier Science B.V. All rights reserved.

Keywords: Magnetoresistance; Thin films—trilayer; Tunneling

Interest in ferromagnetic–insulator–ferromagnetic (F–I–F) trilayer structures, for use as magnetic tunnel junctions (MTJ), remains strong as their high magnetoresistance [1,2] (MR) holds great promise for sensor, magnetic random-access memory [3,4] and read-head [5] applications [6]. To reduce the response time, the current technological drive is to decrease the MTJ resistance-area product (RA) by using thinner insulating barriers—a trend that has reopened the question of how to rule out the presence of direct metal–metal contacts through barrier pinholes. At first sight, one might expect such contacts to drastically decrease the MR by effectively shunting the spin-dependent current with a spin-independent one. However, recent findings of up to 300% ballistic MR in magnetic nanocontacts [7–10] suggest that pinholes might enhance the device performance by simultaneously contributing to its high MR and low RA. To optimize the performance of F–I–F structures, one hence needs to know whether conduction is dominated by tunneling or not.

In the 1960s and 1970s, a set of criteria (so-called Rowell criteria) was formulated to identify single-step elastic electron tunneling in superconductor–insulator–superconductor (S–I–S) structures [11]. Unfortunately, only three of these criteria may apply when neither of the electrodes superconducts: (I) exponential thickness dependence of the conductance (or resistance), (II) non-linear behavior of either the current–voltage relation ($I-V$) or the differential conductance vs. bias ($\mathrm{d}I/\mathrm{d}V - V$) that should be well fitted by a rectangular [12] or trapezoidal [13] barrier model, and (III) weak insulating-like temperature dependence of the conductance (or resistance). In the MTJ literature, the second criterion is most commonly used.

As a complement to the global electrical transport approach, on which the Rowell criteria are based, one may probe the insulating-barrier quality locally by using microscopic techniques. Recent advances include 'hot spot' detection using STM and conductive AFM [14] and Ballistic Electron Microscopy [15]. However, typical RA values of about 10^3–$10^5\,\Omega\,\mu\mathrm{m}^2$ for MTJs and $10^{-3}\,\Omega\,\mu\mathrm{m}^2$ for contacts imply that an Ångström-sized contact can dominate the transport properties of a micron-sized MTJ, obviously putting very high demands on microscope resolution. In order to relax the resolution requirement, the size of a pinhole can be

*Corresponding author. Tel.: +1-480-755-6513; fax: +1-480-755-5502.
E-mail address: JohanAkerman@motorola.com (J.J. Åkerman).

0304-8853/02/$ - see front matter © 2002 Elsevier Science B.V. All rights reserved.
PII: S0304-8853(01)00712-0

augmented using electrodeposition, such that an optical microscope suffices for its detection [16]. Recently, X-ray photoelectron spectroscopy was also used to search for pinholes in tunnel junctions [17]. However, the convenience of a fast, global, and non-destructive approach that can be readily applied to the device in its final package should not be understated, as evidenced by the prevalence of the Rowell criteria in the literature.

In the first part of this work, we put the three remaining Rowell criteria to the test, using a superconducting electrode as a probe of the barrier, and show that neither the first nor the second criteria are in fact reliable as indicators of tunneling dominating the conduction in F–I–F structures. On the other hand, the third criterion—a weak insulating-like temperature dependence of the conductance—is indeed reliable and should hence, *always* be used to rule out pinholes through the insulating barrier.

In the second part, we investigate the behavior of MTJs with and without shorts through the barrier, and based on our experimental results, we suggest additional criteria that can be used to determine whether an insulating barrier is pierced by a metallic conductive path.

The first Rowell criterion is a consequence of the evanescent nature of the electron wave function inside the insulator barrier region. Within the Wentzel–Kramers–Brillouin approximation, the characteristic length scale of the decaying wave function amplitude is $z_0 = \hbar/\sqrt{8m\phi}$, where m is the electron's effective mass and ϕ the barrier height. Using the bare electron mass and $\phi = 1$ eV, one gets $z_0 \sim 1$ Å. As we have shown in the following, the exponential thickness dependence is only a necessary, but not sufficient, criterion, since other conduction mechanisms may also lead to an exponential thickness dependence, with similar characteristic decay length (order of 1 Å).

Consider a perfectly smooth metallic surface on top of which we randomly deposit cubes of insulating barrier material up to an average height μ, measured in a number of monolayers. The random nature of the deposition introduces surface roughness, which for a very thin layer results in incomplete coverage, i.e. barrier pinholes. As the insulator thickness at different locations follows a Poisson distribution, the probability that any given metal area remains uncovered is proportional to $\exp(-\mu)$. Alternatively, the fraction of the total metal area that will be uncovered by the insulator is also given by $\exp(-\mu)$. If a metal is deposited on top of the insulator, and only classical conduction is allowed, the perpendicular conductivity of this trilayer will be directly proportional to the pinhole area, and hence proportional to $\exp(-\mu)$. As a consequence, not only tunneling but also an entirely classical conduction mechanism can lead to an exponential thickness dependence, now with a characteristic length scale of exactly one atomic layer thickness. It is hence clear that the first Rowell criterion cannot be used to rule out the existence of barrier pinholes. The above argument can be extended to include both non-zero insulator conductance and surface mobility of the deposited insulating blocks, without changing significantly the exponential behavior in the thickness regime of interest (5–20 Å) [18].

The second Rowell criterion is the most commonly used test of tunneling in the literature on MTJs. One either fits $I-V$ data to the Simmons' model [12] for a rectangular barrier shape or $\mathrm{d}I/\mathrm{d}V - V$ data to the Brinkman–Dynes–Rowell (BDR) model [13] for a trapezoidal barrier shape. If reasonable barrier parameters are obtained, one concludes that the F–I–F structure has an integral tunneling barrier.

To test this criterion, we used the Superconductor–Insulator–Ferromagnetic (S–I–F) trilayers that allow us to apply the more solid Rowell criterion of the experimental detection of the characteristic BCS superconducting density of states. All samples had the following general structure: a DC-sputtered superconducting Nb/Al bilayer bottom electrode, an insulating aluminum oxide barrier, and a DC-sputtered Fe top electrode that was subsequently capped with Al to prevent oxidation. Details of the sample fabrication are reported in Ref. [19].

Typically, two classes of samples were fabricated with, respectively, high and low oxidation levels of the insulating barrier. The results presented in the first part of this paper were obtained on samples A and B, which are representative samples from each class. Prior to the deposition of the top electrode, the Nb/Al bilayer of sample A was stored in air for several days and subsequently exposed to an oxygen glow discharge ($P_{O_2} = 350$ mTorr, 350 V DC bias) for 1.5 h to ensure formation of a thoroughly oxidized pinhole-free aluminum-oxide barrier. Consequently, a high room-temperature RA product of 8.2 MΩ μm^2 was achieved over a junction area of 1000×300 μm^2. The oxidation level of the barrier in sample B was limited by exposing it to air for only 45 min before top electrode deposition, resulting in RA = 0.45 MΩ μm^2 over a junction area of 50×50 μm^2. Standard AC (1 kHz) differential conductance measurements as a function of the DC bias were carried out from liquid-helium temperatures to room temperature, using a conventional balanced bridge. $I-V$ data were obtained by numerically integrating the $\mathrm{d}I/\mathrm{d}V - V$ data.

Fig. 1a presents the normal-state $I-V$ data for sample A, together with a fit to the Simmons' formula [13] with fitted barrier parameters $d = 2.89$ nm and $\phi = 0.49$ eV. The inset shows the differential conductance data for the same sample with a fit to the BDR model yielding essentially the same barrier parameters, since the $\mathrm{d}I/\mathrm{d}V - V$ data do not exhibit any significant

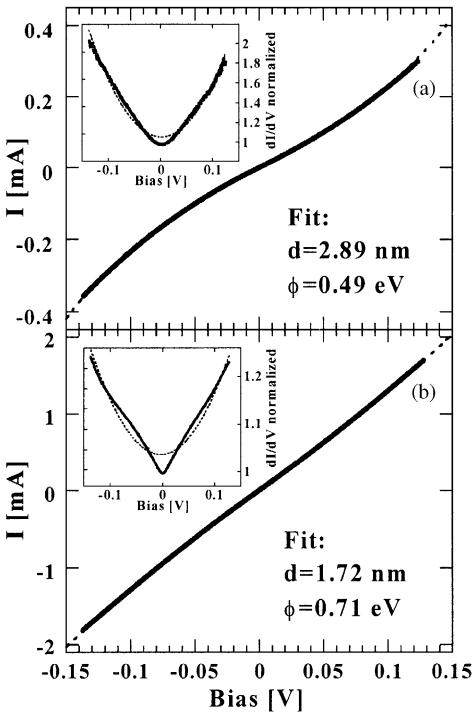

Fig. 1. (a) $I-V$ data for sample A above T_c fitted with the Simmons model (dashed line). Inset: differential conductance data for the same sample fitted with the BDR model (dashed line). (b) Same for sample B.

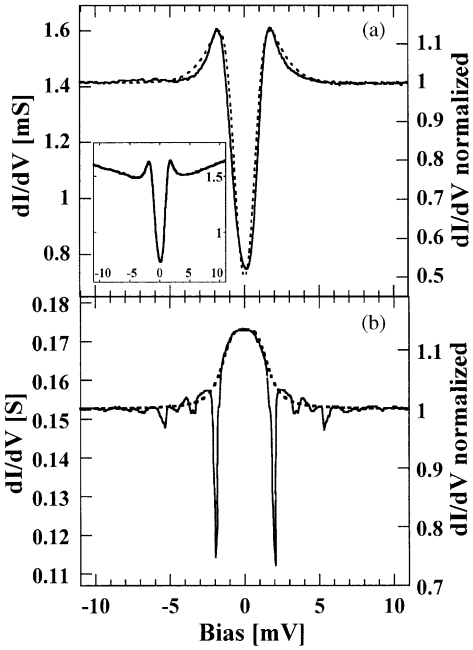

Fig. 2. Differential conductance data for sample A (a) and B (b) at $T = 4.2$ K. The inset in (a) shows the original data before subtraction of the quasi-parabolic background. The dashed line in (a) corresponds to a thermally smeared ($T = 5$ K) theoretical BCS tunneling curve for a gap of $\Delta = 0.84$ meV. The dashed line in (b) is a fit to the extended BTK model, with $Z = 0$, $\Delta = 0.84$ meV and $P = 43.4\%$.

asymmetry. Fits of $I-V$ data to the Simmons' model always appear to be more convincing, since such fits effectively neglect much of the higher sensitivity of the differential conduction measurement and, in particular, ignore any zero-bias anomalies about $V = 0$. We, nevertheless, choose this representation since this is the most common way to test for tunneling in F–I–F structures. Fig. 1b shows the normal-state $I-V$ and conductance data for Sample B with fits to Simmons's and the BDR formulae, respectively. Equally reasonable barrier parameters of $d = 1.72$ nm and $\phi = 0.71$ eV were obtained. It is noteworthy that the shorter oxidation time of sample B does translate into a thinner barrier width. Had these samples been of the F–I–F type, we would have concluded that both samples were good tunnel junctions with pinhole-free barriers, and moreover, we would have argued that by varying the oxidation time, we can vary the barrier thickness.

However, these conclusions are immediately invalidated when the samples are cooled below T_c of the Nb electrode. Sample A shows a typical signature of single-step elastic electron tunneling into a superconducting gap at finite T: a *reduced* conductance at $V = 0$ and two symmetric maxima just outside the gap (inset in Fig. 2a). Once the quasi-parabolic background is subtracted, the experimental data can be well fitted (dashed line) by a theoretical $\mathrm{d}I/\mathrm{d}V - V$ curve based on a BCS density of states with a gap of $\Delta = 0.84$ meV and thermal smearing corresponding to a temperature of 5 K. This proves that sample A has an integral insulating barrier and that the tunneling current dominates the perpendicular conduction through the trilayer. The extracted gap value is lower than that of bulk Nb (1.5 meV) as electrons tunnel into Al, being superconducting through proximity to the Nb film. The $\mathrm{d}I/\mathrm{d}V$ data for Sample B, on the other hand, are entirely different and, in particular, show a 13.7% conductance *increase* in the superconductor gap region (Fig. 2b). Thus, tunneling *is not* the dominating conduction mechanism in this trilayer. Instead, this behavior is consistent with Andreev Reflection [20] (AR) at a highly transmissive superconductor–normal metal (S–N) interface. Indeed, from a fit to a model based on an extended Blonder–Tinkham–Klapwijk theory (BTK) [21,22], a spin polarization of $P = 43\%$ of the Fe electrode, in excellent agreement with literature values [23,24], a gap of $\Delta = 0.84$ meV, and a zero Z value of the point contact can be extracted. We also observe a number of resistivity spikes outside the gap, as is often observed in S–N nanocontacts [25,26]. Altogether, these observations prove that Sample B suffers from a short

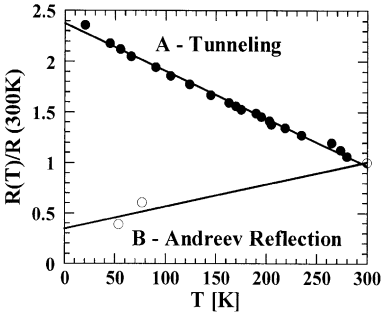

Fig. 3. Temperature dependence of the zero-bias resistance for the two categories of samples.

between the Fe and Nb electrodes. Similarly, all other samples that we studied in detail could also be classified as clear tunnel junctions or clear S–F contacts. Regardless of the existence of a pinhole in the barrier, equally good fits of the $I-V$ data could be made to Simmons's formula at $T > T_c$. We must, therefore, conclude that a fit above T_c cannot be used as a criterion to ascertain whether or not a tunneling barrier is free of pinholes. Both the first and the second Rowell criteria should thus be used with great caution.

The third criterion is tested in the same way. All samples were divided into true tunnel junctions (tunneling into a BCS density of states) or trilayers with contacts through the barrier (AR). The temperature dependence of the zero-bias resistance was then determined for all samples. For example, sample A, being a tunnel junction, shows a weak, insulating behavior, whereas sample B, which contains a short, appears metallic (Fig. 3). After all samples had been tested, we did in fact find a 100% correlation between the temperature dependence of the resistance and the sub-T_c differential conductance data. We hence conclude that a metallic-like temperature dependence of the zero-bias resistance is incompatible with a pinhole-free barrier. To rule out the possibility of a pinhole in the barrier of F–I–F junctions, one should therefore *always* check that the temperature dependence is insulator-like, even if the $I-V$ data can be fitted with reasonable barrier parameters. Similar conclusions have recently been drawn by other groups [27,28]. The observed combination of quasi-parabolic $dI/dV - V$ data and a metallic-like $R(T)$ dependence most likely arises from a competition between the tunneling path and the contact path. As the temperature is decreased, the metallic contact dominates the conduction and gives the observed $R(T)$ as well as the AR below T_c.

It is somewhat disheartening that only a single Rowell criterion can be trusted when testing MTJs, and it would be of great value if a larger set of reliable criteria could be formulated. In an attempt to provide additional tunneling criteria, we have studied the temperature dependence and bias dependence of R and MR of as-prepared MTJs and MTJs that have been intentionally shorted.

Details of the sample fabrication are reported in Ref. [29]. Briefly, the bottom-pinned MTJ material used an IrMn exchange layer, a NiFeCo/CoFe bilayer for the bottom magnetic electrode, and NiFeCo alloy for the top magnetic electrode. The AlO_x tunnel barrier was formed by depositing approximately 10 Å of Al on the bottom electrode followed by oxidation in an RF-produced oxygen plasma to form a junction with an RA of approximately $8\,k\Omega\,\mu m^2$. The wafer was annealed at 250°C to improve the tunnel barrier [30] and then patterned to $10 \times 10\,\mu m^2$ bits by standard lithographic techniques.

Two samples from the same wafer were studied in detail. Originally, both had integral tunneling barriers as determined from the temperature dependence of the resistance. One of the samples, labeled S for 'short', was exposed to a voltage pulse above its breakdown voltage, which induced a short in the barrier and reduced its room-temperature resistance from 53 to 38 Ω. After an initial cool-down to 4.2 K, the same sample was again exposed to a voltage pulse which further reduced R to 25 Ω, and all further measurements on sample S were carried out in this shorted state. Sample J had an MR of 36% at 4.2 K and 23% at RT. From the narrow distribution of same-wafer MR values [3,4], we can assume that sample S had the same MR as J before being shorted.

Fig. 4a shows $R(T)$ for sample J in both the magnetic states. The weakly insulator-like temperature dependence indeed proves that sample J has an integral tunneling barrier and that electron tunneling dominates the conduction in this device. Fig. 4b similarly shows $R(T)$ of sample S for two different number (or sizes) of shorts through the barrier. The open diamond marks the original R of 53 Ω before any short was induced. $R(T)$ of the shorted junction is in all cases weakly metal-like. These results corroborate the validity of $R(T)$ as a reliable criterion for MTJ barrier quality.

The resistance of sample S in the P state is 24.9 Ω at 4.2 K, which corresponds to a short of about 47 Ω in parallel with the original junction. Assuming that the remaining junction area still has an MR of 36%, one expects that $R = 28.4\,\Omega$ in the AP state, which is very close to the observed value of 27.9 Ω. The expected MR is 14%, again very close to the experimentally observed value of 12%. The short hence does not seem to introduce any significant MR on its own that would add to the tunneling MR [7–10].

Fig. 5 shows $dV/dI - V$ for samples J and S in the AP state at 4.2, 90 and 155 K, respectively. Again $R(T)$ is completely different for the two samples. It is interesting to note that the evolution of $R(T)$ with

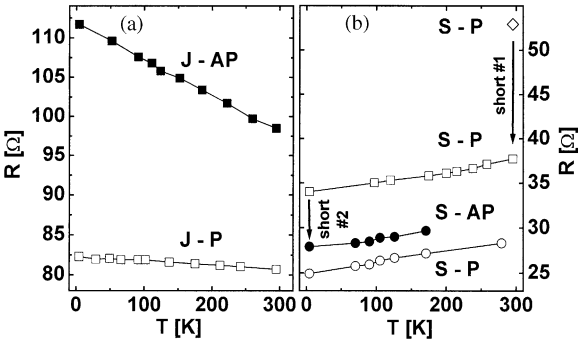

Fig. 4. (a) $R(T)$ for sample J in both the antiparallel (■) and parallel (□) magnetic states. (b) same for sample S. Open diamond and arrow show R before and after the first short was introduced. Small contact, P state (□); large contact, AP state (●); large contact, P state (○).

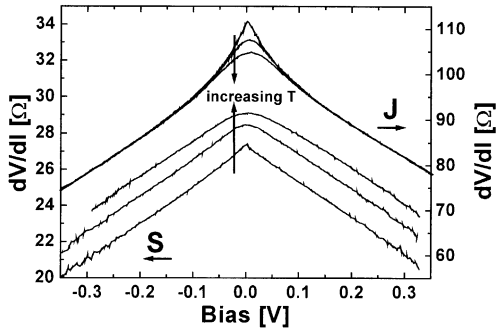

Fig. 5. Differential resistance vs. applied bias at 4.2, 90 and 155 K respectively. Three top curves: sample J; three bottom curves: sample S.

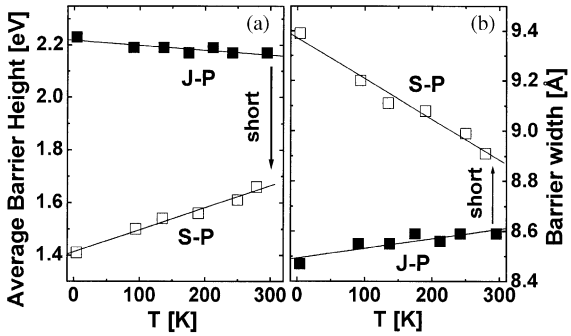

Fig. 6. Average barrier height (a) and barrier width (b) vs. T for sample J (■) and S (□) in the parallel state. Straight lines are guides to the eye.

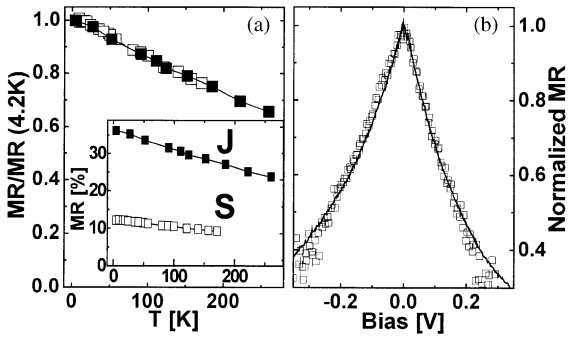

Fig. 7. (a) T dependence of the normalized differential MR for sample J (■) and S (□). Inset: same data before normalization. (b) Bias dependence of the differential magnetoresistance of sample J (—), and S (□).

increasing bias is entirely different for the two junctions. Above an absolute bias level of about 0.1 V, sample J exhibits a vanishing temperature dependence. The metal-like $R(T)$ of sample S on the other hand is equally apparent at all bias levels and consistent with a short with no bias dependence.

The short will inevitably alter the *apparent* barrier parameters that are extracted from fits to either the Simmons [12] or the BDR [13] model. It is important to note that the *apparent* barrier parameters are just fitting parameters with no real physical significance, especially for sample S. While the fitted barrier parameters of sample J are only weakly temperature-dependent, both the barrier thickness and the barrier height of sample S vary more strongly with temperature (Fig. 6). The short effectively decreases the apparent barrier height and increases the apparent barrier width. As the resistance of the short decreases with decreasing temperature, its influence on the apparent barrier parameters further increases. The observation of a sudden drop of the fitted barrier height accompanied by an *increase* in the fitted barrier width, in a study of barrier parameters vs. insulator thickness, would consequently mark the first appearance of a pinhole through the insulator.

Fig. 7 shows the temperature dependence of the normalized MR of both samples J and S. Although the absolute MR decreased from 36% to 12%, as the short was introduced, the overall shape of the temperature dependence is still virtually identical. The short has an equally insignificant effect on the bias dependence of the MR (Fig. 7b). The shape of the MR dependence is, hence, of very limited use as an indicator of the barrier quality.

A striking difference between samples J and S is the noise level at finite bias. While our measurement does not detect any bias dependence in noise level for sample J, sample S shows a strongly increasing noise for $|V| > 0.2$ V. The additional noise in sample S is likely to come from Johnson noise over the metallic contact. A contact with $RA = 10^{-3}\,\Omega\,\mu m^2$ has to sustain a huge current density of $2 \times 10^{10}\,A\,cm^{-2}$ at 0.2 V, which will raise the local temperature, hence the increase in noise with increasing bias.

Other shorted junctions also showed greater instability above 0.2 V, and R could change dramatically both to lower and higher values if a very high bias was applied. If the bias is continuously increased, a weakly shorted junction will eventually break down completely at about 0.5 V, leaving a fully shorted device with very low R and MR. Again, the huge current density is expected to lead to electromigration, which may alter the size of the contact.

Based on our experimental results above, we suggest the following criteria to ascertain whether a magnetic–insulator–magnetic trilayer contains a short in parallel with the insulator: (i) metal-like $R(T)$ at all bias levels, (ii) decreasing fitted barrier height and increasing fitted barrier thickness for decreasing T, (iii) increased junction noise at finite bias, and (iv) increased junction instability at finite bias.

In conclusion, we have scrutinized the Rowell criteria that are routinely used to verify whether tunneling dominates the perpendicular conduction in F–I–F trilayers. We have found that neither the exponential thickness dependence of the conductivity nor reasonable fits of the non-linear transport properties can be reliably used as criteria for MTJ barrier quality. Of the Rowell criteria that have previously been assumed to apply to F–I–F structures, only the temperature dependence of the conductivity remains a good test to uniquely identify tunneling. Additional criteria for a shorted barrier have been formulated based on studies on MTJs with integral as well as intentionally shorted tunneling barriers. A short is found to introduce artificial temperature dependences of both the resistance and the apparent fitted barrier parameters. While the short does reduce the MR of the MTJ, it has a surprisingly weak effect on the general shape of both the temperature dependence and the bias dependence of the MR. One cannot, hence, base any strong criterion on the MR behavior of a MTJ. Finally, there is a dramatic increase in noise and sample instability once a short has been introduced through the barrier.

We are indebted to Y. Ji and C.L. Chien for fitting our AR data to their extended BTK model. The work at UC—San Diego was supported by DARPA, ONR and the US-DOE. The work at Motorola Labs was partially funded by DARPA. R.E. thanks the John Simon Guggenheim Memorial Foundation, and CONACYT-MEXICO. D.A.R. is a Cottrell Scholar of Research Corporation.

References

[1] J.S. Moodera, L.R. Kinder, T.M. Wong, R. Meservey, Phys. Rev. Lett. 74 (1995) 3273.
[2] T. Miyazaki, N. Tezuka, J. Magn. Magn. Mater. 139 (1995) L231.
[3] S. Tehrani, J.M. Slaughter, E. Chen, M. Durlam, J. Shi, M. DeHerrera, IEEE Trans. Mag. 35 (1999) 2814.
[4] S. Tehrani, B. Engel, J.M. Slaughter, E. Chen, M. DeHerrera, M. Durlam, P. Naji, R. Whig, J. Janesky, J. Calder, IEEE Trans. Mag. 36 (2000) 2752.
[5] J. Zhang, Data Storage 5 (1998) 31.
[6] S.A. Wolf, D. Treger, IEEE Trans. Mag. 36 (2000) 2748.
[7] N. García, M. Muñoz, Y.-W. Zhao, Phys. Rev. Lett. 82 (1999) 2923.
[8] N. García, M. Muñoz, Y.-W. Zhao, Appl. Phys. Lett. 76 (2000) 2586.
[9] G. Tatara, Y.-W. Zhao, M. Muñoz, N. García, Phys. Rev. Lett. 83 (1999) 2030.
[10] G.G. Cabrera, N. García, unpublished.
[11] J.M. Rowell, in: E. Burnstein, S. Lundqvist (Eds.), Tunneling Phenomena in Solids, Plenum, New York, 1969, p. 273.
[12] J.G. Simmons, J. Appl. Phys. 34 (1963) 1793.
[13] W.F. Brinkman, R.C. Dynes, J.M. Rowell, J. Appl. Phys. 41 (1970) 1915.
[14] W. Wulfhekel, M. Klaua, D. Ullmann, F. Zavaliche, J. Kirschner, R. Urban, T. Monchesky, B. Heinrich, Appl. Phys. Lett. 78 (2001) 509.
[15] W.H. Rippard, A.C. Perrella, R.A. Buhrman, Appl. Phys. Lett. 78 (2001) 1601.
[16] R. Schad, D. Allen, G. Zangari, L. Zana, D. Yang, M. Tondra, D. Wang, Appl. Phys. Lett. 76 (2000) 607.
[17] X. Batlle, B.J. Hattink, A. Labarta, J.J. Åkerman, R. Escudero, I.K. Schuller, unpublished.
[18] D.A. Rabson, B.J. Jönsson-Åkerman, R. Escudero, C. Leighton, S. Kim, I.K. Schuller, J. Appl. Phys. 89 (2001) 2786.
[19] B.J. Jönsson-Åkerman, R. Escudero, C. Leighton, S. Kim, I.K. Schuller, D.A. Rabson, Appl. Phys. Lett. 77 (2000) 1870.
[20] A.F. Andreev, Sov. Phys. JETP 19 (1964) 1228.
[21] G.E. Blonder, M. Tinkham, T.M. Klapwijk, Phys. Rev. B 25 (1982) 4515.
[22] G.J. Strijkers, Y. Ji, F.Y. Yang, C.L. Chien, J.M. Byers, Phys. Rev. B 63 (2001) 104510.
[23] R.J. Soulen Jr., J.M. Byers, M.S. Osofsky, B. Nadgorny, T. Ambrose, S.F. Cheng, P.R. Broussard, C.T. Tanaka, J. Nowak, J.S. Moodera, A. Barry, J.M.D. Coey, Science 282 (1998) 85.
[24] R. Meservey, P.M. Tedrow, Phys. Rep. 238 (1994) 173.
[25] P. Xiong, G. Xiao, R.B. Laibowitz, Phys. Rev. Lett. 71 (1993) 1907.
[26] P.S. Westbrook, A. Javan, Phys. Rev. B 59 (1999) 14606.
[27] U. May, K. Samm, H. Kittur, J. Hauch, R. Calarco, U. Rüdiger, G. Güntherodt, Appl. Phys. Lett. 78 (2001) 2026.
[28] U. Rüdiger, R. Calarco, U. May, K. Samm, J. Hauch, H. Kittur, M. Sperlich, G. Güntherodt, J. Appl. Phys. 89 (2001) 7573.
[29] J.J. Åkerman, I.K. Schuller, J.M. Slaughter, R.W. Dave, Appl. Phys. Lett., 79 (2001) 3104.
[30] J.M. Slaughter, E.Y. Chen, R. Whig, B.N. Engel, J. Janesky, S. Tehrani, J. Metals, JOM-e 56, http://www.tms.org/pubs/journals/JOM/0006/Slaughter/Slaughter-0006.html (2000).